**Machine learning for design, phase transformation and mechanical properties of alloys**

J F Durodola*

**School of Engineering, Computing and Mathematical Sciences, Faculty of Technology, Design and Environment. Oxford Brookes University, Wheatley Campus, Wheatley, OX33 1HX**

**Abstract**

Machine learning is now applied in virtually every sphere of life for data analysis and interpretation. The main strengths of the method lie in the relative ease of the construction of its structures and its ability to model complex non-linear relationships and behaviours. While application of existing materials have enabled significant technological advancement there are still needs for novel materials that will enable even greater achievement at lower cost and higher effectiveness. The physics underlining the phenomena involved in materials processing and behaviour however still pose considerable challenge and yet require solving. Machine learning can facilitate the achievement of these new aspirations and desires by learning from existing knowledge and data to fill in gaps that have so far been intractable for various reasons including cost and time. This paper reviews the applications of machine learning to various aspects of materials design, processing, characterisation, and some aspects of fabrication and environmental impact evaluation.

Keywords: Machine learning, artificial neural network, materials design, processing, characterisation, fabrication, environment

*Correspondence author. Tel.: 44-1865-483-501; E-mail address: jdurodola@brookes.ac.uk (J.F.Durodola)

## 1.0 Introduction

Kaplan and Haenlein [1] described Artificial Intelligence (AI) as systems with ability to correctly interpret external data, to learn from such data, and to use those learnings to achieve specific goals and tasks through flexible adaptation. The roots of the concept aimed at developing systems with capabilities to mimic human cognition involving processes such as learning and problem solving [2]. Much earlier aims included creation of computer systems that can reason and draw useful conclusions about the world around. According to Patterson [3] AI began in earnest with the emergence of modern computers in the 1940s and 1950s. Arthur Samuel who carried out a lot of work on making computers learn from their experience, from 1949 to 1960s, is credited as a pioneer in AI [4] . He used the game of checkers as platform for a lot of his work. From 1961 to 1963 Feigenbaum and Feldman [5] collated 20 articles from other pioneers such as Arthur Samuel, Alan Turin, Marvin Minsky and others in book titled Computers and Thought. Patterson [3] projected in 1990, that AI may be the most important development of this century. While the full depth of earlier expectations have not been realised, AI has indeed become pervasive in all aspects of life, technology, industry, finance, business, commerce, retail, wellbeing and entertainment.

Machine Learning (ML) is a subset of AI in which the system learns from information that is available without a prior knowledge of the relationship between the input and the output. It enables associations to be formed between input and output without first establishing the nature or type of functional forms that govern the relationship. This statement can be expatiated further by supposing that some environmental observations ***x*** are related to outputs ***y*** by some unknown function **g** so that ***y = g(x).*** A Machine Learning model is developed starting with an initially arbitrary machine model function ***F(x,w)*** which with training approximates the function ***g(x)*** very well so that in the end ***F(x,w)*** $\approx \boldsymbol{g}(\boldsymbol{x})$. The variables ***w*** are adjustable enablers in the model that allows a relationship to be formed. During training, a loss function such as ***L(y; F(x,w))*** is used to indicate the discrepancy between predictions and the expected values ***y***. A quadratic loss function such as the Euclidian distance between the prediction and the actual values ***y***, i.e. $L(\boldsymbol{y}; \boldsymbol{F}(\boldsymbol{x}, \boldsymbol{w})) = \|\boldsymbol{y} - \boldsymbol{F}(\boldsymbol{x}, \boldsymbol{w})\|^2$ is commonly used[6].

ML is a broad field consisting of many aspects. Table 1 is illustrative of the breakdown of the field [7]. In broad terms, ML can be divided into three main categories depending on the learning approach used in the training of the system. These approaches are supervised, unsupervised and reinforcement learning methods. In the supervised learning method, the system is set up initially as a model that has capacity to learn but is undeveloped or 'ignorant' until it is trained. The training process involves presenting the model with a set of input and corresponding output data such as **x** and **y** for which association or relationship needs to be made. The presentation of the correct output data matching the input data to the model during training is what is referred to as supervision. The training process involves iterative or adaptive changes to the model until it has learnt to correctly make association or form a relationship between the input and the output data to a reasonable degree of accuracy as highlighted in the foregoing. The model having been trained is tested on previously unseen set of input and output data. The performance of the model is tested by how well or correctly, it predicts the output corresponding to the inputs used in the test. The accuracy achievable depends on the complexity or the degree of nonlinearity of the relationships between the input and output data. Supervised learning is generally used for classification or regression purposes. The former refer to discrete output while the latter refer to continuous output. In the context of materials science, classification variables could be the number and type of phases formed given a set of alloy contents and processing conditions used. Regression results, in the same context, could be temperatures at which phase transformations begin, the volume fraction of the phases formed, etc.

In unsupervised learning, the (ML) model is only presented with input data. In the course of training, the model learns how to cluster the information presented into groups. Of course, the model require guidance such as how many groups should be formed. In reinforcement learning, the model is trained on a task by allowing it to take random actions with the aim to achieve a goal. The model is given a reward for success and penalty for failure. Through this process, it learns over many iterations the best ways to achieve the goals. The suggestion that there is no supervision is conceited in the sense that the environments are actually designed by humans to enable the ML systems to learn. There are many ML models categorised as supervised, unsupervised and reinforcement learning methods as illustrated in Table 1. Under each category are a number of sub classifications such as support vector machine (SVM), neural networks, decision trees, random forest, deep neural networks etc. Of all models, artificial neural networks (ANN) seems to be the most versatile being used on its own or in conjunction with other models. This review concentrates mainly on the use of ANN. Artificial neural networks (ANN) are mathematical models us to enable complex or generally non-linear relationships to be formed between input and output data. There are a number of neural network architectures as illustrated in Figure 1. A number of the architectures look similar but the bases of the algorithms for the implementation are different. Van Veen and Leijnen [8] provides an extensive list of various types of neural network architecture and a brief description of each.

Materials design, processing, and characterisation modelling have been challenging in terms of development of hard rules of relationships between input factors and parameters and product output. This presently prevail because of the limited knowledge of all interacting factors and the difficulty of controlling processing conditions at different sites in the material. For example, alloying is a dynamic process consisting of heat and mass transfer, chemical phenomena, phase transformations and complex multiphase interactions involving solid, liquid and gaseous phases. The knowledge of the physics of matter influences such as electromagnetic effects is presently incapable for developing the laws that governing relationships and where descriptors are known at any scale, solutions of the equations are still intractable. Although publications on the use of AI commenced in the early 1960s [5] the earliest publication on the use of AI and ML applied to materials appear to have started in the late 1980s and early 1990s [9-11]. These early work by Chryssolouris and Guillot [9], Rangwala and Dornfeld [10] Sathyanarayanan et al [11] focused on the use ML for the optimisation of machining processes. The next surge of work in the late 1990s witnessed application of ML to various areas of material processing, properties and machining. Bhadeshia [12] contains an excellent review of these works up to 1999.

As highlighted in the foregoing, forming non-linear relationships as required in materials science can be quite challenging[13]. ML has been shown to have capacity to form non-linear relationships between inputs and outputs in many fields. One of the greatest appeals of the approach is the ease of the construction of the models, albeit sufficiently large sets of development data has to be available. This review highlights the application of ML to various aspects of materials design, processing, characterisation and fabrication that has been published. ANN is one of the most powerful and widely applied methods of ML [14-16]. Some background about this method is first presented before applications of ML in various areas of materials are reviewed from literature.

**2.0 Background on Artificial neural network**

Artificial neural networks are mathematical models inspired by the functioning of neurons in the brain. There are a number of different network architectures such as single layer perceptron, radial basis network, recurrent neural network and multilayer perceptron, etc. Of these, the multi-layer perceptron network is the most versatile in terms of scope of application. Figure 2 shows an example of a multi-layer perceptron having three layers. This has an input layer, a hidden layer and an output

layer. Although many outputs are possible from an ANN as in Figure 2(a) a single output as in Figure 2 (b) reduces the complexity of the function to be minimised in forming the model. Each layer in the ANN structure has a number of neurons as numbered in the Figure 2. The neurons in the first layer take one input data each, while the neurons in the hidden and output layers each take weighted data from all the neurons in the preceding layer as illustrated by the arrows in the Figure. The total input to a hidden or output layer neuron *j* receives propagated information from all the neurons *i* in the preceding layer as described in equation (1) and the output from the neuron which transfer information out of it is described by equation (2).

$$x_j = \varphi(x_i, w_{ij}) \tag{1}$$

$$y_j = \emptyset(x_j) \tag{2}$$

where φ is described as the propagation function [17] that rationalises the inputs from all the neurons *i* to neuron *j* in the next layer and $\Phi$ which is known as the transfer or activation function relates the propagate value received by the neuron *j* to the output from it. The term $w_{ij}$ is known as the strength of the connection between the neurons *i* that feed into the neurons *j*. We have used the index *i* here to represent neurons in a preceding layer and *j* to represent the neurons in the following layer. The propagation function is a linearly weighted sum of all the information from the nodes *i* added to the bias value for neuron *j* as described by equation (3). This function is also called an adder or linear combiner [6]. There are various forms of the activation or the transfer function. Typical functions are binary threshold, Heaviside step function, Fermi function (or logistic function) $1/(1+e^{-x})$, and hyperbolic tangent [6, 17, 18]. A sigmoid function is described in equation (4). A linear transfer function equation (5) is often used as the transfer function for the output layer.

$$x_j = \theta_j + \sum_i w_{ij}\, x_i \tag{3}$$

$$y_j = \frac{1}{1+\exp(-\sigma x_j)} \tag{4}$$

$$y_j = \theta_j + x_j \tag{5}$$

In equation (3), $\underline{\vartheta_j}$ is the bias value associated with the neuron *j* and is a parameter that alters the shape of the sigmoid function, the inverse of it is also called a temperature parameter [17]. The sigmoid function in equation (4) limits the values passing to the next neuron to be $\in [0,1]$ and its form simplifies the minimisation formulation for the backpropagation process for weight adjustments towards model convergence.

**2.1 Training**

The weights $w_{ij}$ are initially set up randomly to be $\in [0,1]$. This arbitrary start means the output from equations (4) and (5) will not match the expected output values in a supervised learning training paradigm. The process of minimising the error involves iteratively modifying the weights $w_{ij}$ by adding a corrective incremental value $\Delta w_{ij}^k$ during the training process. Suffice to indicate that $\Delta w_{ij}^k$ can be

positive or negative. One of the easily understood training method is the gradient descent method, which is described by equations (7) and (8).

$$w_{ij}^{k+1} = w_{ij}^{k} + \Delta w_{ij}^{k} \tag{7}$$

$$\Delta w_{ij}^{k} = -\alpha \, \nabla E(w_{ij}) \tag{8}$$

The parameter α in equation (8) is known as the learning parameter and the rest of the term on the right hand side of equation (8) is the gradient of the error function *E* with respect to the weights. The weights of the hidden layer are similarly modified in a backpropagation process. The aim of these process is to attain minimal *E* which in absolute terms is achieved when $\nabla E(w_{ij})$=0. An approximation to this minimisation is deemed to be achieved when in many cases the mean square error after an iteration number *k* is deemed to be small enough provided overfitting [12] is not simultaneously taking place. The mean square error can be expressed as in equation (9)

$$E(\boldsymbol{w}^{k}) = \frac{1}{2N}\sum_{q}^{N}[t_q - y_q^k]^2 \tag{9}$$

where $t_q$ and $y_q^k$ are the target value and predicted value for the input data set *q* and *N* is the total number of data sets used for the training. After training, the performance of an ANN on unseen test data is often expressed by the quality of the fit or the correlation between predicted and actual values. It is common as can be seen in the articles reviewed in this work from sections 4 to 10, to use the coefficient linear least square fit, m, or the Pearson regression coefficient, R or $R_{X,Y}$ given in equations (10) and (11) as indicators of performance.

$$m = \mathrm{cov}(X,Y) / \mathrm{var}(X) \tag{10}$$

$$R_{X,Y} = \frac{E[(X-\mu_X)(Y-\mu_Y)]}{\sigma_X \sigma_Y} \tag{11}$$

where in these equations, *X* and *Y* represent actual and predicted values respectively and $\mu$, $\sigma$, *E, var,* and *cov* denote statistical mean, standard deviation, expectation, variance and covariance respectively. While the R value expresses alignment, the $R^2$, value which is the square of the R value indicates the proportion of the total variability in the predicted value *Y* that is accounted for by the actual values *X [19]*. It is also described as a measure of the extent to which the total variation of the dependent variable *Y* is explained by the regression [20].

**3.0 Efficacy of ML and ANN results**

As highlighted in the foregoing machine learning models approximate the underlining solutions to the problems of interest. The efficacy of the solution of a ML model depends on several factors. The initial or proposed structure of the ML model ***F(x,w)*** should be capable of representing the problem. With the exception of deep learning ML models, the input data should be fundamental bases that govern or at least apparently govern the problem. In materials ***x*** = ***x****(c,T,t,G,Q,h,σ,ε, ….)* that is, it could consist of inputs such as *c,T,t,G,Q,h,σ,ε* which are elemental composition, temperature, time, and Gibbs free energy, diffusion constant, and mechanical working parameters; stress, strain, respectively depending on the specific problem. The input is usually kept to the minimum relevant possible in order to

facilitate quick development of the model. The data should be of sufficient quantity and quality to allow good coverage of the problem in order for generalization of the solution over the domain to be possible. ML models are statistically based because they depend on finite sets of data that are available for the development of the models and the initial values of ***w***, which are arbitrary.

The efficacy of ML predictions can be enhanced by systematic evaluation of several feasible functions ***F(x,w)*** and the selection of a set of best performing models among those built and tested. In the case of ANN, the structure of ***F(x,w)*** is defined by the architecture of the network. The development of the model is carried out by monitoring three simultaneous processes, which are training, validation, and testing. Available data is divided into three parts for these processes. The aim in all three processes is to minimise the error prediction. The cut-off is made at the stage when validation error starts to increase even though training error carries on decreasing. Usually a number of models are developed in this way to form a committee of machines [21, 22]. During application, some form of averaging of results of the committee members is carried out.

Having highlighted the backgrounds to ML and its potentials to support materials design, processing and characterisation and the basis for good models, the next sections in the paper are focussed on a cross section of reported applications of ML in various areas of materials science and development.

**4.0 Alloy design modelling**

Alloying presents an almost infinite number of design possibilities for new materials with different characteristics. Cantor [23] using combination analysis and Stirling's approximation for large numbers estimates that about $10^{279}$ different materials can be produced using 80 non-radioactive elements or components on the periodic table and assuming material differentiation specification of 0.001%. Of course, not all possible element combinations can lead to materials with desirable properties. Some combinations can however lead to materials that significantly outperform existing ones. This rarity of a good outcome makes experimental alloy design testing with combination of elements without guidance to be impractical in terms of costs and the remote chances of success. Virtual or modelling search in aid of development of new alloys, which is on many scales more feasible, has been of interest by various research and development laboratories and groups. A Material Genomic Initiative (MGI) for global competitiveness in the USA to double the speed and reduce the cost of discovery, development and deploying of new advanced materials is a major investment in materials science [24, 25]. This process has been made possible by the availability of methods such as CALPHAD [26-30] that allow thermophysical and thermomechanical analysis of a given combination of elements to be used to determine thermodynamic properties of the product. Having obtained these, information about predicted phases and volume fraction can be used to predict mechanical properties. Details of some specific applications of ML for alloy design are highlighted in the following.

Yin et al defined a High Entropy Alloy (HEA) as a random alloy with five or more components, often near equi-composition, that often exhibit excellent mechanical properties[31]. Cantor [23] provides an excellent review of HEAs, especially Cantor alloys [23, 32], and his discovery of the field. Although his pioneering work was carried out in the 1970s, the first publication from his group was not until year 2004[32]. Yeh [33] who also worked in the field independently coined the HEA reference to the alloys. Figure 3 [34] illustrates the difference between conventional and HEAs in terms of structure. Menou et al [35] used Genetic Algorithm (GA) for the multi-objective design search for HEAs that are light and strong. The analysis aimed to identify new alloys with a composition that will result in highest

substitutional hardening, single-phase stability and low-density alloys with all the objectives simultaneously satisfied. Genetic algorithm analysis was used with data obtained through data mining and data obtained from the application of CALPHAD for thermophysical and thermochemical studies to assess the thermodynamic properties of all phases in a system. Altogether, 63019 families of possible alloys composed of a minimum of 5 out of 16 elements (Al, Co, Cr, Cu, Fe, Hf, Mn, Mo, Nb, Ni, Ru, Ta, Ti, V, W and Zr) were considered; of these, 3155 alloys were found on the multiobjective Pareto face of the multidimensional property optimisation studies. From these, $Al_{35}Cr_{35}Mn_8Mo_5Ti_{17}$(at %) which was chosen for experimental validation presented the highest known Vickers hardness of 6.45 GPa (658 $H_V$) for a material with a density below 5.5 g/cm$^3$. Wang et al [36] also used thermodynamics modelling to design new Ni-base alloys in a fast throughput manner. The use of ML in this work focussed primarily on image recognition for the characterisation of the microstructure as opposed to modelling approach for materials design.

Yu et al[37] and Ruan et al[38] used ML learning together with CALPHAD for accelerated design of novel W free high strength Co based superalloys with extremely wide γ/γ' region, low mass density and higher temperature capabilities. These alloys are used primarily for petro-chemical, power generation, turbine and aerospace industries. The works aimed to meet multi objective property optimisation purposes. Yu et al[37] predicted the dependence of γ' precipitate area on 21 alloy components Co, Ni Al, Ru, W, Re, Ta, Fe, Nb, Hf, Ti, Zr, V, Sc, B, Ge, Cr, Ga, Si, Ir, Mo as well as the process parameters, which were, aging temperature and aging time. The outcome in this case was classification obtained by using support vector machine (SVM) and random forest (RFC) methods. The solvus temperature, $T_{\gamma'}$, was predicted using regression analysis for which the input were the 21 alloy elements. The regression analysis were carried out using ordinary least squares (OLS). Vector regression (SVR), artificial neural network (ANN) and random forest regression (RFR) ML methods. The data samples were 458 from existing published data. In the end, the RFC decision tree was identified as being the better option for the classification work and the random forest regression, RFR, method gave best prediction for the regression work.

Wen et al [39] used experimental design for the development of high entropy alloys (HEA) with $Al_xCo_yCr_zCu_uFe_vNi_w$ components with the constraint x + y + z + u + v + w = 100%. The data obtained from this was used to train ML based models. The ML methods considered, included regression tree method, back propagation ANN and radial basis function kernel. The best performing models in terms of excellent prediction were identified and used these to design optimal HEA for high hardness. Dey et al [40] used a combination of ANN and Genetic Algorithm (GA) for the design of 2000, 6000 and 7000 series aluminium alloys. Figure 4 [41] shows a flowchart typical of integration of ANN in a GA analysis. The main elements of the GA analysis are mutation, cross over and selection processes. In the case of [40], the ANN was trained using 259 data set from reference [42]. The inputs were chemical composition and processing parameters and the output were mechanical properties. The input consisted of weight % Si, Fe, Cu, Mn, Mg, Cr, Ni, Zn, Zr, Ti, solutionising temperature, ageing temperatures, ageing time, mechanical testing temperature and cold work as illustrated in Figure 5. The outputs consisted of yield and tensile strengths and % elongation. The Pearson correlation coefficient, R, between predicted and actual value ranged between 0.961 and 0.991. Figure 6 shows the plot of ANN predicted values [40] against experimental values from [42] for the yield stress (YS) and ultimate tensile stress (UTS). The GA designed alloy shows promise. Mohanty et al [43] similarly used a combination of ANN and GA for the design of cold rolled IF steel sheets with optimized tensile properties. The data in the ANN developed were obtained from a Tata Steel production source over

six months at Jamshedpur. The composition of the alloy, the finish rolling temperature, coiling temperature of hot strip mill, percentage cold deformation, batch annealing parameters and skin pass mill elongation were taken as input parameters. The networks were trained to predict tensile strength, yield strength and % elongation. The R-values ranged from 0.805 to 0.95. The GA design result output was, however, not manufactured. In reference [44] Dutta et al used ANN and GA for the design of dual phase steels to optimise strength and ductility. The data used for the ANN development consisted of 464 sets of test results from various sources including references [45-48]. The input data to the ANN were %wt of elements such as C, Mn, Si, Cr, V, B, Cu, Mo, Nb and Ti in Fe and processing parameters such as intercritical annealing temperature and time, intermediate and step quenching processes. The outputs for the ANN training were yield and tensile strengths, uniform and total elongation, yield ratio and strain hardening exponent. The R-value for the predictions ranged from 0.8679 to 0.9143. The optimal DP steel design was then carried out by using GA with ANN providing the objective values for the multi-objective optimisation study. The optimal steels were, however, not produced or tested.

Conduit et al[49] used ANN and CALPHAD and existing material data to predict an optimal combination of cost, density, γ' phase content and solvus, phase stability, fatigue life, yield stress, ultimate tensile strength, stress rupture, oxidation resistance, and tensile elongation for a nickel base superalloy. The inputs were composition and heat treatment. The tool predicted a new nickel-base polycrystalline alloy that offered an ideal combination of properties, seven of which were experimentally verified. Wu et al [50] used machine learning to recommend affordable new Ti alloy with bone-like modulus of elasticity. The elements used in the alloy design in addition to Ti included Ta, Mo, Sn, Zr and Nb. Two ANN models were designed in the work, one to predict the martensitic transformation temperature (Ms Temperature) and the other to predict the Young's of the alloy. The input to both ANNs were the alloy composition by weight in percentage (%). The ANN for the Young's modulus prediction used 164 published composition data and the modulus property of the alloys as the target. The second ANN used 112 data sets of both composition and Ms Temperature. The performance of the models were assessed using the root mean square error of the prediction. The Young's modulus values used in the study had been obtained using different test techniques such as tensile, resonance, compression, nano-indentation and bending methods. The performance of the ANN was found to be much improved when results from one test technique alone was used in the training and validation.

**4.1 Element content estimation**

Rodriguez et al [51] used various ML methods such as neural networks, decision tree and k-means neighbourhood analysis to estimate the carburizing level of HT steels produced using pyrolysis furnaces. Experimental pulse-echo ultrasonic tests were performed in HP steel pipes are used. Three types of carburisation cases designated as non-carburised (NC), low carburised (LC) and high carburised (HC) steels were analysed. The level of carburisation affected the ultrasound waveform. The signals from ultrasound tests were digitized using discrete Fourier transform (DFT) to extract features used for inputs to the ML models. Only the first 100 coefficients from the DFT were used as inputs. The training was performed on 600 signals from tests on the three carburisation cases. The diagonal values of confusion matrices for the ANN, decision tree and KNN methods showed good agreement with the values of 99, 87 and 100% respectively.

**5.0 Kinetics and diffusion**

The knowledge of properties for kinetic analysis is required for heat treatment and design process involving creep. ML can be used directly or in conjunction with CALPHAD methods for the determination of these properties. Direct approaches are based on availability of existing data for training. Some specific applications are summarised in the following to highlight details of application.

Strandlund [52] used ANN to increase the speed of thermodynamic calculations for kinetic simulations. Detailed simulation of diffusion process for a given alloy system could be carried out by coupling a kinetics to a thermodynamics software such as CALPHAD or Thermo-Calc. The thermodynamic properties obtained from the latter can be time consuming to obtain because of the iteration and optimisation steps involved. He proposed the use of this intensive software at a few state conditions to obtain the thermodynamic properties and ANN is then trained on these data and used to predict properties under other state conditions as may be required. As few as 100 grid state points were required to train the ANN. The diffusion of a binary (Fe-Ni) and a ternary (Fe-C-Si) alloy systems at 1400 K and 1323 K were analysed in this way. The use of ANN reduced the computational time by a factor of 70 in the binary alloy case. In the ternary alloy case, a total time of 3.8 hours was taken instead of 4.8 hours for each time step and a total of 1538 time steps taken for the direct use of the thermodynamic software.

In a remarkably wide scope study Zeng et al[53] used ML to predict the diffusion activation energies of N, O, B and C in bcc, fcc, and hcp metals using gradient boosting and regression tree decision method. In the study, 648 impurity – host systems were considered. These were generated from 94 elements on the periodic table and 4 impurities. In the modelling, 21 features were identified as having influence in the determination of activation energy. These included electronic properties of the elements such as atomic and Mendelev numbers, atomic radii, mass, and valence electron; bcc, FCC and hcp structure properties such as lattice constant, ratio, total energy and vacancy formation energy. Some others include melting and Debye temperatures, thermal coefficient of expansion and shear modulus. The number of trees used in the study varied from 50 to 150 in steps of 25 with 75 being found as optimal. The trees were trained on the known systems and the corresponding values of the activation energy. The diffusion activation energies of 554 new binary impurity-host systems were then predicted. The $R^2$ value between the known 94 systems' values used in the study and predicted values was 0.897.

**6.0 Phase transformation curves**

Phase transformation curves are useful for the design of heat treatment procedures for achievement of required microstructures and properties. Figure 7 shows an example of a continuous cooling transformation diagram of a Ti-6Al-5Mo-5V-1Cr-1Fe alloy showing the various phases that will be achieved under different cooling rates[54].

Malinov et al [55] used ANN to predict the time temperature transformation (TTT) plots for titanium alloys. A multilayer feedforward backpropagation method was used. The influence of Al, V, Mo, Sn, Zr, Cu, Fe O and Cr on the kinetics of the transformation of binary, ternary and more complex titanium alloys was modelled. The input sample data, 189 in all, was collected from published data. Four separate networks were formed for the nose point, the upper and lower parts of the TTT diagram and the martensite start transformation temperature predictions. The work concentrated on predicting

the transformation start time only given a relative temperature change above or the below the nose point. The input in all cases were the concentration of the alloy elements Al, V, Mo, Sn, Zr, Cu, Fe O and Cr. In the case of the prediction of the nose temperature and the time, these parameters were the output for the training of the ANN. For the prediction of the upper part of the curve, there were 10 pairs of temperature and time as illustrated in Figure 8 and similarly for the lower part of the curve. The results agreed with an R correlation coefficient of over 0.9 generally. Dobrzanski et al [56] focussed on the use of radial basis ANN to predict the influence of cooling rate and composition on phase transformation characteristics of ACAlSi7Cu cast alloys. Three cooling rates of 0.2, 0.5 and 1 $^{o}$C/s were considered and the compositions of Si, Fe, Cu, Mn, Mg, Zn and Ti were varied subjected %Sr + %Ni + %Sn + %Pb + %Na + %Ca ≤ 0.3. Different ANNs were built to predict 10 types of outputs including four characteristic, one microscopy measurement and 5 mechanical properties. Some of the predictions included temperature and others such as α aluminium nucleation temperature, dendrite coherent temperature, end of solidification temperature, grain size, yield stress, elastic limit and hardness. The Pearson correlation coefficient between prediction and experimental results was stated to vary from 0.89 to 1.00. It was not clear if the authors meant R or $R^2$ coefficient. In reference [57], ANN was used for the prediction of bainite volume fraction content in low carbon steels. The inputs were composition consisting of C, Si, Mn, Ni, Mo, Cr, V and Fe as well as isothermal transformation temperature and time on a TTT diagram. A vector of 437 input data was obtained from Matsuda and Bhadeshia [58], Caballero et al [59] and Chester et al [60]. Surprisingly, 25 ANNs were trained using only 35 input vectors and the performance of the ANNs were checked using the remaining 402 vectors. The performance of the networks for the prediction of bainite volume fraction was high with very low error levels.

**7.0 Mechanical properties characterisation**

Mechanical properties such as elasticity constants, plastic flow, yield and ultimate tensile strength, elongation, % reduction area, hardening coefficients and exponents, fatigue resistance, creep and others such as impact energy absorption are important requirements for efficient and effective engineering design of components. These properties are predominantly determined by mechanical testing and can be very expensive in terms of time and cost, especially the high temperature properties. Furthermore, every alloy has its own set of properties, which is different from others even if the main elements in family of an alloy are the same. It is, therefore, helpful to have a means to be able to use ML to make prediction based on any knowledge of an alloy that is available such as element composition, processing history such as heat treatment and mechanical working. There have been a number of efforts in this direction using ML to determine the mechanical properties in the literature. Some approaches include use of density functional approach to support the development of predictive ML models [61].

**7.1 Flow stress modelling**

Pagan et al [62] used unsupervised machine learning method to analyse X-ray diffraction data to identify a reduced number of embedded coordinates that characterise plastic flow during thermos-mechanical loading of alloys. They carried out in-situ X-ray measurements during the uniaxial loading of additively manufactured Inconel superalloy IN625 specimens. The experiments included 38 instances during a loading rate of 10 nm/s corresponding to a strain-loading rate of 0.03 /s. The diffraction peak measurements were transformed into column vectors given a total of 38 x 7.5 million

data points. By using locally linear embedding ML method, they identified a reduced number of dimensions that characterise the evolution of defects such as dislocation flow and pile up at obstacles. Three of the dimensions identified were shown to be related to dislocation density, pile up and their rates when plotted against loading strain.

The phase transformation of TC18 titanium alloy (wt%) of 5.16 – Al − 4.92Mo − 4.96V − 1.10Cr − 0.98Fe −(bal.) Ti, in the σ + β regime as well as the flow behaviour were studied in [63]. Particularly, ANN, strain compensated Arrhenius and Hensel-Spittel type constitutive models were used to characterise the flow. Strain rates between 0.001 to 0.1 /s and temperatures between 1033 and 1123 K were considered. The inputs to the ANN were temperature, strain rate, and strain while the output was flow stress. In all, 2000 experimental test data were used in the study. The training was based on 60% of the data and 40% was used for the testing. The Pearson correlation coefficient R of the three methods were 0.9971, 0.9866 and 0.9739. ANN gave the best predictions of the three methods. Quan et al [64] also modelled the flow stress of Ti–6Al–2Zr–1Mo–1V alloy over strain range of 0.01 to 10 /s and a wide temperature range 1073 to 1323 K. The data used in the study was obtained from 24 experimental flow stress results under the strain rate and temperature ranges highlighted. An improved Arrhenius model in which the material properties were traditionally taken as constant were re-expressed as functions of strain. The ANN performed better and gave nearly perfect correlation with experimental data although the ANNs were however trained for specific strain rates only rather than generalised across all strain rates.

**7.2 Static mechanical properties**

Some examples of readily accessible publications covering elasticity constants, yield and ultimate tensile strength, elongation, % reduction area, hardening coefficients and exponents, and others such as impact energy absorption include [61, 65-76]. The types of alloys covered in this work include carbon steels, austenitic stainless steels, die steels, maraging steels, and aluminium, copper, molybdenum, nickel, titanium based alloys. Generally, as highlighted in the foregoing, the input into the predictive models include chemical composition (as many as 19 elements in some cases), cooling curve characteristics and parametrised mechanical working conditions. Details of some specific applications are given in what follows.

In reference [77] the mechanical properties of group III type cast copper alloys Cu–Sn–Pb–Zn–Ni (wt%) were predicted using ANN. The properties predicted were yield strength, tensile strength and elongation. The number of inputs are the composition by weight % of the elements was 5, the number of hidden neurons in the hidden layer was 10 and 3 for the properties highlighted. The composition and properties used for the training were obtained from ASM handbook [78]. The data used was however, limited to 21 from the reference and only 8 were used for testing. The $R^2$ value for the prediction of strength, yield and elongation for the ANN test stage ranged from 0.9872 to 0.9996. In [79, 80] a database of 308 titanium alloys from Matweb and a handbook of titanium alloys [80] were used for the training of ANN to predict tensile and yield strengths, modulus of elasticity and biocompatibility measures. The alloy composition by weight % of Mo, V, Al, Zr, Nb, Ta, Mn, Cr, Fe, Sn, Si, O, N, C, H, Ni, Y, Pd and Ru were varied and thermomechanical processing conditions such as solution treatment, ageing, annealing and forging digitised and used as input variables. The Pearson coefficient, R, for the prediction in the ANN testing stage for yield strength, tensile strength, modulus of elasticity were 0.8434, 0.8276, 0.9284 respectively. The biocompatibility analysis was carried out

using recursive-partitioning approach and gave 100% correct prediction. Sun et al [81] used ANN developed experimental data from forging and heat treatment experiments to predict the mechanical properties of the Ti–6Al–4V. The input variables were forging temperature, degree of deformation, annealing temperature and annealing time. The output variables from various ANNs were ultimate tensile strength, yield strength, elongation and reduction in area. The ANN architecture used was 4-14-4. The R-value varied from 0.9330 to 0.9930. Ghamarian et al [82] Used a combination of ANN, GA and Monte Carlo method to develop phenomenological equations with 20 unknown variables for the prediction of yield strength of α+β processed Ti-6Al-4V with accuracy of 96%.

**7.3 Fatigue characteristics, loading, damage and failure**

Fatigue resistance and associated damage is one of the most difficult material characteristics to predict [12]. As with other fields, there have been applications of ANN to different aspects of fatigue analysis. Some researchers [83-87] considered the use of ANN to construct SN models. Bhadeshia [12] explored the application of ANN to assist with the establishment of relationships between material and loading variables especially for crack propagation life prediction. Typical examples of S-N curves at different levels of probability of failure can be found in reference [88] and crack growth rate plots, at different stress ratios, R, conditions can be found in reference [89].

Arty [83] used 304 sets of experimental data for steel alloys to develop ANN for SN prediction. The factors included stress ratio R (not to be confused with Pearson correlation coefficient also designated as R), types of loading, specimens shape, ultimate tensile strength, used strength, fatigue notch factor, $K_f$, and constant amplitude condition. Pujol et al [84] developed ANN based on a series of 232 sets of cumulative loading data to predict probability of damage values. Others such as Iacoviello et al [85] used ANN to predict the effect of stress ratio on fatigue crack propagation for a duplex steel. There has been an attempt to use ANN method to predict fatigue damage under cumulative loading condition[86] as an alternative to the Miner's rule approach [89]. The inputs to the network were the fatigue limit, strength coefficient, a, and strength experiment, b, point of inflection Nd, maximum stress amplitude Sa, severity of spectrum, V, sequence length, $H_i$, and irregularity factor, I. A database of 825 experimental tests, more than half of which were carried out on ferrous materials was used in the study. The model appeared to have performed better than using the classical Miners rule approach [89]. By using an ANN approach, Kang et al [90] showed that faster prediction can be made under multiaxial random loading conditions. The effect of different sequences of temperature on fatigue life was recently predicted by Martinez and Ponce [87] using ANN. There has not been much on the use of ANN for random loading fatigue analysis. Kim et al [91] used ANN to determine the probability density function for double block spectral loading. They obtained better prediction than those in references [92-96].

**7.4 Random loading fatigue analysis**

Recently, the author and colleagues developed ANN models [21, 97-99] for the analysis of random loading fatigue problems. In the initial work, Gaussian distribution random fatigue loading was analysed. Contrary to prevailing tendencies, generalized approach was developed to relate fatigue damage to different forms of spectrum loading and material properties that cover a broad conceivable range of metal alloys. The input to the neural networks were the zeroth to fourth frequency spectral moments (with the exception of the third) of the power spectral density, strength and fatigue material

properties. The output was the fatigue damage corresponding to the inputs. The architecture of the neural network was 7– 35-1. Up to 50000 data sets was generated in the study. Training was based on 70% of the data, 15% was used for validation and the last 15% was used for the testing of the ability of the neural networks to make predictions and to demonstrate that there had been no overfitting [12]. The models developed were tested with fresh unseen data. The results obtained for prediction compared with known data agreed with linear least square coefficient of fit which were generally greater than 0.990. In the second phase of the work [98], analysis of random loading fatigue including the effect of mean stress was analysed. It was found that additional input into neural networks were required. Some of these parameters included a Goodman's factor for accounting for the effect of the mean stress in a global sense and parameters including maximum and minimum stress ratios with respect to the ultimate tensile strength. The number of inputs required in this case were 11 in total. The architecture of the neural network was 11–35-1. The $R^2$ value was generally over 0.990. In the third phase of the work [21], published experimental data by the society of automotive engineers SAE was used to verify the performance of the ANN models that were developed in the first two phases [100]. The ANN model which included the effect of the mean stress performed well in the analysis of the SAE data. In the study in reference [99], it was realised that a lot of components are actually subjected to non-Gaussian random loading. This lead to further developments of the ANN models. In this case, additional inputs were further found necessary to make good predictions of fatigue damage. The extra inputs included skewness $S_k$ and kurtosis $K_r$ parameters. These are given by equations (12) and (13).

$$S_k(x) = E\left[\left(\frac{x-\mu}{\sigma}\right)^3\right] \tag{12}$$

$$K_r(x) = E\left[\left(\frac{x-\mu}{\sigma}\right)^4\right] \tag{13}$$

where μ and σ are the mean and standard deviation of the signal $x$. The results demonstrated the ability of the ANN to make better predictions overall for various forms of random fatigue loading problems.

**7.5 Crack propagation**

Shi et al [101] used ANN to develop a link between stress intensity factor, electrochemical corrosion potential, temperature, conductivity, pH, flow velocity and degree of sensitization with crack growth rate (CGR) as the output for type 304SS steel. The number of data sets obtained from 26 different sources including references [102-105] was 280. The ANN architecture was 6-25-20-20-1. Most of the predicted results were included within 95% confidence level on a log-log relationship. The ANN developed in this study were further verified in [106]. Shi et al [107] again similarly used ANN for the prediction of primary water stress corrosion crack growth rates in Alloy 600. The crack growth predicted from the trained ANN were in good agreement with the experimental data that were used for evaluation purposes.

**8.0 Time dependent deformation**

Effort has been made to also use ML methods to predict time dependent deformation behaviour. References [108-117] are some examples of ML based publications covering creep. The main input requirements for the ML model were alloy composition, static mechanical properties [114], heat treatment and prior mechanical working parameters, microstructure details such grain size, mechanical loading stress level applied, prior creep strain and temperature. In some specific component assessment cases, heat flux into an assembly were included as input[110, 111]. The output from the ML models were mostly % creep strain and creep strain rate. Most studies concentrated on nickel and titanium base alloys. A few typical application of ML to creep are summarised in the following.

Hou et al [113] carried out a typical creep predictive analysis. The input in this study covered content, heat treatment, grain size, temperature and the loading stress. The output predicted in the study was creep rupture life. The architecture of the ANN was 25-7-1. The number of data set used was 220 and the number of data set used for testing was 80. The R value for the prediction between predicted and actual was 0.9330. In [109], ANN was used to predict the time dependent deformation of nickel-based superalloys 276 and 617. The inputs used included the alloying content, the loading stress and the operating temperature. The temperature levels considered were 750 and 850 degrees centigrade. The load levels were set at 10% and 25% the yield stress. The output from the ANN were percentage creep strain and creep strain rate. The number of samples used here was very low, 20 data sets, the approach was characteristic of creep prediction. In [110] and [111], ML was used for the analysis of nuclear reactor pipes. The input in this analysis included alloy content, ultimate tensile strength, yield stress, % elongation, temperature and heat flux. The ANN architecture was 9-12-1. This study used 703 sets, 539 were used for training and 164 sets were used for testing. The R correlation Factor achieved was 0.9875. In reference [114], ML was used to predict the scatter of results at a given load condition. This study was based on nickel base alloy 738 LC. Reference [116] considered the prediction of life under low cycle creep - fatigue interaction. The ANN architecture was 5-4-1. The inputs were strain rates of testing, strain amplitude, and cold work. The output was the range of scatter in fatigue life.

**9.0 Metal composite properties**

Adithiyaa et al[118] developed a k-nearest neighbour – grey wolf optimisation model for predicting the mechanical properties of a squeeze cast aluminium alloy based metal matrix composite. The AA 2219 alloy was reinforced with TiC as the primary reinforcement materials and $Al_2O_3$ and $Si_3N_4$ as the secondary reinforcement materials. The processing parameters varied included stirring speed and time, feed rate, squeeze pressure, die and melt temperatures. The KNN method was used to classify the products into groups. The grey wolf method was used to identify the optimal performance parameters for prediction purposes. The properties predicted from the processing parameters were ultimate tensile stress, impact energy, and hardness. The trends of the prediction followed those of experimental results.

**10.0 Fabrication and environmental impact**

**10.1 Welding characterisation**

Pouraliakbar et al [119] used ANN to predict the hardness of the heat affected zone (HAZ) of API X70 HSLA pipeline steels. The inputs to the network were chemical composition and tensile strength. The data set was based on 104 experimental test results. The submerged arc welding processes on the hardness of the HAZ was considered. The elements included in the steel were C, Ti, Nb, Cr, Mo, Ni, V and Nb. The input layer consisted of 8 neurons including yield strength, tensile strength, % elongation and five sums of the %wt compositions from the combination of the elements such as V, Ti, Nb; Cr, Mo, Ni, Cu; Nb, V and two based on different interpretations of carbon content. The $R^2$ value of prediction of microhardness varied from 0.8295 to 0.9587.

Lakshminarayanan et al [120] used response surface method (RSM) with ANN methods to predict the tensile strength of friction stir welded AA7039 aluminium alloy joints. The elements in the composition of the alloy were Zn, Mg, Mn, Fe, Si, Cu, Cr, Ti and Al. The process variables considered as input for effect on joint strength were rotational speed, welding speed and axial force. Three levels of values were considered for each input parameter. Design of experiment selection based on three factors, three-level, and central composite face centred method was used in determining the combination of the parameters. The $R^2$ value for the RSM and ANN methods for predictions were 0.9699 and 0.9918 respectively showing better performance for the latter.

### 10.2 Surface texture and machining

Thankachan et al [121] studied prediction of surface roughness and material removal rate using ANN. The material in this case was aluminium alloy with various concentrations of Mg, Si, Fe, Sn, Mn, Cu, Cr, Zn, Ni, Ti, and SiC. The varying proportions of Sn was from 5 to 20 % wt in steps of 5%. The EDM material was a 0.25 mm brass wire and deionised water was used as the dielectric medium. The inputs to the ANN were the weight percentage of SiC and Sn; pulse on time (PON), pulse off time (POFF) and wire feed rate (WFR). The outputs were materials wear rate and surface roughness. The ANNs were assessed using the mean absolute error measures. They found feedforward backpropagation ANN architecture 5-7-1 and 5-10-1 to be optimal for the prediction of material removal rate and surface roughness measures respectively.

### 10.3 Environmental impact modelling

The work of [122] used genetic programming (GP) machine learning to develop models for the prediction of the impact of electric discharge machining settings on environmental and manufacturing performance. In the study a chromium tool steel was machined using copper and kerosene was used as the dielectric medium[123]. The setting considered included peak current, pulse duration, dielectric level and flushing pressure. The environment impact was assessed in terms of the energy used, dielectric consumption, relative tool to wear ratio and the manufacturing performance was assessed by quality measures such as surface roughness and process material removal rate. Two GP models based on Akaike information criteria (AIC)[18, 124] and predicted residual sum of squares as fitness functions were considered. The AIC model performed better in general.

## 11.0 Challenges and prospects

The main challenges with machine learning include the selection of appropriate structure for the approximation model ***F(x, w)*** and the establishment of the enabling parameters ***w*** to ensure that

the best model has been achieved. Machine learning models are as good as the quantity and quality of the data and features used for their training. The challenge with this is the uncertainty of knowing if the data available adequately covers the full bases of the problem of interest and thereby reduce probabilities of misinterpretation and prediction. The challenge is further expanded by the uncertainties of how much data is required. While hundreds may be required for some problems, thousands and millions may be required in others depending on the complexity of the problem and the range of the variables involved. Furthermore, the cost of generating data in some cases can be extremely prohibitive. It was concerning to find in the review that some enthusiastic machine learning analyses were carried out with obviously scanty data. This practice is highly misguided and unadvisable.

The prospects for developments and applications of machine learning in materials is vast. A single universal model is unlikely to be achievable just as it has not been possible with closed-form solutions. It is, however far easier to flexibly build machine learning models for problems in a regimented form that can be coupled together to solve higher-dimensional problems. A balance also needs to be struck in this process to avoid unnecessary scale reduction where higher is possible. There appears to be limited use, so far, of deep learning machine learning approach that may help with microstructure characterization. This is a good area for prospects for automation of quality control for example during material processing.

**12.0 Conclusions**

The paper has presented highlights of the backgrounds of machine learning to aid in its understanding and appropriate application. The review of previous and recent works carried out covers various aspects of materials design, processing, characterisation and fabrication. The forms of input and outputs involved in the various areas and the predictive abilities of machine learning achieved are highlighted. While machine learning is a powerful tool, its statistical basis and none closed-form structure, leaves some probability of misinterpretation and prediction. It has nevertheless proved to be extremely versatile and helpful in every area of materials analysis.

**References**


1. Kaplan, A. and M. Haenlein, *Siri, Siri, in my hand: Who's the fairest in the land? On the interpretations, illustrations, and implications of artificial intelligence.* Business Horizons, 2019. **62**(1): p. 15-25.
2. Russel, S. and P. Norvig, *Artificial intelligence: A modern approach, 2003.* EUA: Prentice Hall. **178**.
3. Patterson, D.W., *Introduction to artificial intelligence and expert systems*. 1990: Prentice-hall of India.
4. McCarthy, J. and E.A. Feigenbaum, *In memoriam: Arthur samuel: Pioneer in machine learning.* AI Magazine, 1990. **11**(3): p. 10-10.
5. Feigenbaum, E.A. and J. Feldman, *Computers and thought*. 1963: New York McGraw-Hill.
6. Haykin, S., *Neural networks: a comprehensive foundation*. 2007: Prentice-Hall, Inc.
7. Fumo, D., *Types of machine learning algorithms you should know.* Towards Data Science, Towards Data Science, 2017. **15**.
8. Van Veen, F. and S. Leijnen, *The neural network zoo.* The Asimov Institute, 2016.
9. Chryssolouris, G. and M. Guillot. *An AI approach to the selection of process parameters in intelligent machining*. in *Proc. of The Winter Ann. Meeting of The ASME on Sensors and Controls for Manufacturing, Chicago, Illinois*. 1988.

10. Rangwala, S.S. and D.A. Dornfeld, *Learning and optimization of machining operations using computing abilities of neural networks.* IEEE Transactions on Systems, Man, and Cybernetics, 1989. **19**(2): p. 299-314.
11. Sathyanarayanan, G., I. Joseph Lin, and M.-K. Chen, *Neural network modelling and multiobjective optimization of creep feed grinding of superalloys.* The International Journal Of Production Research, 1992. **30**(10): p. 2421-2438.
12. HKDH, B., *Neural networks in materials science.* ISIJ international, 1999. **39**(10): p. 966-979.
13. Gerguri, S., et al. *Prediction of brittle failure of notched graphite and silicon nitride bars*. in *Applied Mechanics and Materials*. 2004. Trans Tech Publ.
14. Farley, S.J., et al., *A Neural Network Approach for Locating Multiple Defects*, in *Advances in Experimental Mechanics Vi*, J.M. DulieuBarton, J.D. Lord, and R.J. Greene, Editors. 2008. p. 125-131.
15. Hernandez-Gomez, L.H., et al., *Locating defects using dynamic strain analysis and artificial neural networks*, in *Advances in Experimental Mechanics IV*, J.M. DulieuBarton and S. Quinn, Editors. 2005. p. 325-330.
16. Luna-Aviles, A., et al., *Locating and Classifying Defects with Artificial Neural Networks*, in *Advances in Experimental Mechanics Vi*, J.M. DulieuBarton, J.D. Lord, and R.J. Greene, Editors. 2008. p. 117-123.
17. Kriesel, D., *A Brief Introduction to Neural Networks. dkriesel. com.* Online) http://www. dkriesel. com/en/science/neural_networks (last retrieved 30-10-2015, 2005.
18. Bishop, C.M., *Pattern recognition and machine learning*. 2006: springer.
19. Chatterjee, S. and A.S. Hadi, *Regression analysis by example*. 2015: John Wiley & Sons.
20. Sykes, A.O., *An introduction to regression analysis.* 1993.
21. Durodola, J.F., et al., *Experimental validation of an ANN model for random loading fatigue analysis* International Journal of Fatigue, 2019: p. Accepted.
22. Guo, J.-J. and P.B. Luh, *Improving market clearing price prediction by using a committee machine of neural networks.* IEEE Transactions on Power Systems, 2004. **19**(4): p. 1867-1876.
23. Cantor, B., *Multicomponent high-entropy cantor alloys.* Progress in Materials Science, 2020: p. 100754.
24. Liu, Y., et al., *Machine learning in materials genome initiative: A review.* Journal of Materials Science & Technology, 2020.
25. Jain, A., et al., *Commentary: The Materials Project: A materials genome approach to accelerating materials innovation.* Apl Materials, 2013. **1**(1): p. 011002.
26. Olson, G.B. and C. Kuehmann, *Materials genomics: from CALPHAD to flight.* Scripta Materialia, 2014. **70**: p. 25-30.
27. Liu, Z.-K., *First-principles calculations and CALPHAD modeling of thermodynamics.* Journal of phase equilibria and diffusion, 2009. **30**(5): p. 517.
28. Saunders, N., M. Fahrmann, and C. Small, *The application of CALPHAD calculations to Ni-based superalloys.* ROLLS ROYCE PLC-REPORT-PNR, 2000: p. 803-811.
29. Zhu, J., et al., *Linking phase-field model to CALPHAD: application to precipitate shape evolution in Ni-base alloys.* Scripta Materialia, 2002. **46**(5): p. 401-406.
30. Spencer, P., *A brief history of CALPHAD.* Calphad, 2008. **32**(1): p. 1-8.
31. Yin, B. and W.A. Curtin, *First-principles-based prediction of yield strength in the RhIrPdPtNiCu high-entropy alloy.* npj Computational Materials, 2019. **5**(1): p. 1-7.
32. Cantor, B., et al., *Microstructural development in equiatomic multicomponent alloys.* Materials Science and Engineering: A, 2004. **375**: p. 213-218.
33. Yeh, J.W., et al., *Nanostructured high-entropy alloys with multiple principal elements: novel alloy design concepts and outcomes.* Advanced Engineering Materials, 2004. **6**(5): p. 299-303.
34. Gorsse, S., J. Couzinie, and D. Miracle, *High-entropy alloys: The future of alloying.* 2019.

35. Menou, E., et al., *Computational design of light and strong high entropy alloys (HEA): Obtainment of an extremely high specific solid solution hardening.* Scripta Materialia, 2018. **156**: p. 120-123.
36. Wang, Z., et al., *High throughput experiment assisted discovery of new Ni-base superalloys.* Scripta Materialia, 2020. **178**: p. 134-138.
37. Yu, J., et al., *A two-stage predicting model for γ' solvus temperature of L12-strengthened Co-base superalloys based on machine learning.* Intermetallics, 2019. **110**: p. 106466.
38. Ruan, J., et al., *Accelerated design of novel W-free high-strength Co-base superalloys with extremely wide γ/γ' region by machine learning and CALPHAD methods.* Acta Materialia, 2020. **186**: p. 425-433.
39. Wen, C., et al., *Machine learning assisted design of high entropy alloys with desired property.* Acta Materialia, 2019. **170**: p. 109-117.
40. Dey, S., et al., *Computational intelligence based design of age-hardenable aluminium alloys for different temperature regimes.* Materials & Design, 2016. **92**: p. 522-534.
41. Sun, Y., et al., *Optimization of chemical composition for TC11 titanium alloy based on artificial neural network and genetic algorithm.* Computational Materials Science, 2011. **50**(3): p. 1064-1069.
42. Committee, A.I.H., *ASM Handbook: Properties and selection*. Vol. 2. 1990: Asm International.
43. Mohanty, I., D. Bhattacharjee, and S. Datta, *Designing cold rolled IF steel sheets with optimized tensile properties using ANN and GA.* Computational materials science, 2011. **50**(8): p. 2331-2337.
44. Dutta, T., et al., *Designing dual-phase steels with improved performance using ANN and GA in tandem.* Computational Materials Science, 2019. **157**: p. 6-16.
45. Das, D., P. Chattopadhyay, and N. Bandyopadhyay, *On the Modification of Martensite Morphology in High Martensite Dual Phase Steels for the Improvement of Mechanical Properties.* Journal of the Institution of Engineers(India), Part MM, Metallurgy and Material Science Division, 2003. **84**(2): p. 84-92.
46. Haque, M.E. and K. Sudhakar, *Prediction of corrosion–fatigue behavior of DP steel through artificial neural network.* International Journal of Fatigue, 2001. **23**(1): p. 1-4.
47. Bag, A., K. Ray, and E. Dwarakadasa, *Influence of martensite content and morphology on tensile and impact properties of high-martensite dual-phase steels.* Metallurgical and Materials Transactions A, 1999. **30**(5): p. 1193-1202.
48. Mirzadeh, H., M. Alibeyki, and M. Najafi, *Unraveling the initial microstructure effects on mechanical properties and work-hardening capacity of dual-phase steel.* Metallurgical and Materials Transactions A, 2017. **48**(10): p. 4565-4573.
49. Conduit, B., et al., *Design of a nickel-base superalloy using a neural network.* Materials & Design, 2017. **131**: p. 358-365.
50. Wu, C.-T., et al., *Machine learning recommends affordable new Ti alloy with bone-like modulus.* Materials Today, 2020. **34**: p. 41-50.
51. Rodrigues, L.F., et al., *Carburization level identification in industrial HP pipes using ultrasonic evaluation and machine learning.* Ultrasonics, 2019. **94**: p. 145-151.
52. Strandlund, H., *High-speed thermodynamic calculations for kinetic simulations.* Computational materials science, 2004. **29**(2): p. 187-194.
53. Zeng, Y., Q. Li, and K. Bai, *Prediction of interstitial diffusion activation energies of nitrogen, oxygen, boron and carbon in bcc, fcc, and hcp metals using machine learning.* Computational Materials Science, 2018. **144**: p. 232-247.
54. Sieniawski, J., et al., *Microstructure and mechanical properties of high strength two-phase titanium alloys.* Titanium alloys-advances in properties control, 2013: p. 69-80.
55. Malinov, S., W. Sha, and Z. Guo, *Application of artificial neural network for prediction of time–temperature–transformation diagrams in titanium alloys.* Materials Science and Engineering: A, 2000. **283**(1-2): p. 1-10.

56. Dobrzański, L., et al., *Applications of the artificial intelligence methods for modeling of the ACAlSi7Cu alloy crystallization process.* Journal of Materials Processing Technology, 2007. **192**: p. 582-587.
57. Sidhu, G., et al., *Determination of volume fraction of bainite in low carbon steels using artificial neural networks.* Computational materials science, 2011. **50**(12): p. 3377-3384.
58. Matsuda, H. and H.K. Bhadeshia, *Kinetics of the bainite transformation.* Proceedings of the Royal Society of London. Series A: Mathematical, Physical and Engineering Sciences, 2004. **460**(2046): p. 1707-1722.
59. Caballero, F.G., et al., *Design of advanced bainitic steels by optimisation of TTT diagrams and T0 curves.* ISIJ international, 2006. **46**(10): p. 1479-1488.
60. Chester, N. and H. Bhadeshia, *Mathematical modelling of bainite transformation kinetics.* Le Journal de Physique IV, 1997. **7**(C5): p. C5-41-C5-46.
61. Wang, J., et al., *New methods for prediction of elastic constants based on density functional theory combined with machine learning.* Computational Materials Science, 2017. **138**: p. 135-148.
62. Pagan, D.C., et al., *Unsupervised learning of dislocation motion.* Acta Materialia, 2019. **181**: p. 510-518.
63. Lin, Y., et al., *Phase transformation and constitutive models of a hot compressed TC18 titanium alloy in the α+ β regime.* Vacuum, 2018. **157**: p. 83-91.
64. Quan, G.-z., et al., *Prediction of flow stress in a wide temperature range involving phase transformation for as-cast Ti–6Al–2Zr–1Mo–1V alloy by artificial neural network.* Materials & Design, 2013. **50**: p. 51-61.
65. Desu, R.K., et al., *Mechanical properties of Austenitic Stainless Steel 304L and 316L at elevated temperatures.* Journal of Materials Research and Technology, 2016. **5**(1): p. 13-20.
66. Liu, Y., J.-c. Zhu, and Y. Cao, *Modeling effects of alloying elements and heat treatment parameters on mechanical properties of hot die steel with back-propagation artificial neural network.* Journal of Iron and Steel Research International, 2017. **24**(12): p. 1254-1260.
67. Reddy, N., et al., *Modeling medium carbon steels by using artificial neural networks.* Materials Science and Engineering: A, 2009. **508**(1-2): p. 93-105.
68. Powar, A. and P. Date, *Modeling of microstructure and mechanical properties of heat treated components by using Artificial Neural Network.* Materials Science and Engineering: A, 2015. **628**: p. 89-97.
69. Sun, Y., et al., *Modeling the correlation between microstructure and the properties of the Ti–6Al–4V alloy based on an artificial neural network.* Materials Science and Engineering: A, 2011. **528**(29-30): p. 8757-8764.
70. Malinov, S., W. Sha, and J. McKeown, *Modelling the correlation between processing parameters and properties in titanium alloys using artificial neural network.* Computational materials science, 2001. **21**(3): p. 375-394.
71. Guo, Z. and W. Sha, *Modelling the correlation between processing parameters and properties of maraging steels using artificial neural network.* Computational Materials Science, 2004. **29**(1): p. 12-28.
72. Mahalle, G., et al., *Neural network modeling for anisotropic mechanical properties and work hardening behavior of Inconel 718 alloy at elevated temperatures.* Journal of Materials Research and Technology, 2019. **8**(2): p. 2130-2140.
73. Yang, X.-w., et al., *Prediction of mechanical properties of A357 alloy using artificial neural network.* Transactions of Nonferrous Metals Society of China, 2013. **23**(3): p. 788-795.
74. Zare, M. and J.V. Khaki, *Prediction of mechanical properties of a warm compacted molybdenum prealloy using artificial neural network and adaptive neuro-fuzzy models.* Materials & Design, 2012. **38**: p. 26-31.

75. McBride, J., S. Malinov, and W. Sha, *Modelling tensile properties of gamma-based titanium aluminides using artificial neural network.* Materials Science and Engineering: A, 2004. **384**(1-2): p. 129-137.
76. Fragassa, C., et al., *Predicting the tensile behaviour of cast alloys by a pattern recognition analysis on experimental data.* Metals, 2019. **9**(5): p. 557.
77. Ozerdem, M.S. and S. Kolukisa, *Artificial neural network approach to predict the mechanical properties of Cu–Sn–Pb–Zn–Ni cast alloys.* Materials & Design, 2009. **30**(3): p. 764-769.
78. Castings, A.M.H., *Vol. 15 9th*. 1989, Ed. p. p.771–85.
79. Banu, P.N. and S.D. Rani, *Artificial neural network based optimization of prerequisite properties for the design of biocompatible titanium alloys.* Computational Materials Science, 2018. **149**: p. 259-266.
80. Hussein, A.H., et al., *Biocompatibility of new Ti–Nb–Ta base alloys.* Materials Science and Engineering: C, 2016. **61**: p. 574-578.
81. Sun, Y., et al., *Determination of the influence of processing parameters on the mechanical properties of the Ti–6Al–4V alloy using an artificial neural network.* Computational Materials Science, 2012. **60**: p. 239-244.
82. Ghamarian, I., et al., *Developing a phenomenological equation to predict yield strength from composition and microstructure in β processed Ti-6Al-4V.* Materials Science and Engineering: A, 2016. **660**: p. 172-180.
83. Artymiak, P., et al., *Determination of S–N curves with the application of artificial neural networks.* Fatigue & Fracture of Engineering Materials & Structures, 1999. **22**(8): p. 723-728.
84. Pujol, J.C.F. and J.M.A. Pinto, *A neural network approach to fatigue life prediction.* International Journal of Fatigue, 2011. **33**(3): p. 313-322.
85. Iacoviello, F., D. Iacoviello, and M. Cavallini, *Analysis of stress ratio effects on fatigue propagation in a sintered duplex steel by experimentation and artificial neural network approaches.* International Journal of Fatigue, 2004. **26**(8): p. 819-828.
86. Marquardt, C. and H. Zenner, *Lifetime calculation under variable amplitude loading with the application of artificial neural networks.* International journal of fatigue, 2005. **27**(8): p. 920-927.
87. Jimenez-Martinez, M. and M. Alfaro-Ponce, *Fatigue damage effect approach by artificial neural network.* International Journal of Fatigue, 2019. **124**: p. 42-47.
88. Nishijima, S., *Statistical fatigue properties of some heat-treated steels for machine structural use*, in *Statistical Analysis of Fatigue Data*. 1981, ASTM International.
89. Dowling, N.E., *Mechanical behavior of materials: engineering methods for deformation, fracture, and fatigue*. 2012: Pearson.
90. Kang, J.-Y., et al., *Neural network application in fatigue damage analysis under multiaxial random loadings.* International journal of fatigue, 2006. **28**(2): p. 132-140.
91. Kim, Y., H. Kim, and I.-G. Ahn, *A study on the fatigue damage model for Gaussian wideband process of two peaks by an artificial neural network.* Ocean Engineering, 2016. **111**: p. 310-322.
92. Wirsching, P.H. and M.C. Light, *Fatigue under wide band random stresses.* Journal of the Structural Division, 1980. **106**(7): p. 1593-1607.
93. Zhao, W. and M.J. Baker, *On the probability density function of rainflow stress range for stationary Gaussian processes.* International Journal of Fatigue, 1992. **14**(2): p. 121-135.
94. Benasciutti, D. and R. Tovo, *Spectral methods for lifetime prediction under wide-band stationary random processes.* International Journal of Fatigue, 2005. **27**(8): p. 867-877.
95. Tovo, R., *Cycle distribution and fatigue damage under broad-band random loading.* International Journal of Fatigue, 2002. **24**(11): p. 1137-1147.
96. Dirlik, T., *Application of computers in fatigue analysis*. 1985, University of Warwick.
97. Durodola, J., et al., *A pattern recognition artificial neural network method for random fatigue loading life prediction.* International Journal of Fatigue, 2017. **99**: p. 55-67.

98. Durodola, J.F., et al., *Artificial neural network for random fatigue loading analysis including the effect of mean stress.* International Journal of Fatigue, 2018. **111**: p. 321-332.
99. Durodola, J., *Artificial neural network for Gaussian and non-Gaussian random fatigue loading analysis.* Proceedings of the Institution of Mechanical Engineers, Part C: Journal of Mechanical Engineering Science, 2019. **233**(23-24): p. 7525-7544.
100. Ramachandra, S., et al., *Experimental validation of an ANN model for random loading fatigue analysis.* International Journal of Fatigue, 2019.
101. Shi, J., J. Wang, and D.D. Macdonald, *Prediction of crack growth rate in Type 304 stainless steel using artificial neural networks and the coupled environment fracture model.* Corrosion science, 2014. **89**: p. 69-80.
102. Chung, P., et al., *Environmentally controlled crack growth rate of AISI 304 stainless steel in high temperature sulfate solutions.* Corrosion, 1985. **41**(3): p. 159-168.
103. Hale, D., *The effect of BWR startup environments on crack growth in structural alloys.* 1986: p. 44-49.
104. Andresen, P., *Fracture mechanics data and modeling of environmental cracking of nickel-base alloys in high-temperature water.* Corrosion, 1991. **47**(12): p. 917-938.
105. Andresen, P.L., *Effects of temperature on crack growth rate in sensitized type 304 stainless steel and alloy 600.* Corrosion, 1993. **49**(9): p. 714-725.
106. Shi, J., et al., *Customization of the coupled environment fracture model for predicting stress corrosion cracking in Alloy 600 in PWR environment.* Corrosion Science, 2018. **139**: p. 58-67.
107. Shi, J., J. Wang, and D.D. Macdonald, *Prediction of primary water stress corrosion crack growth rates in Alloy 600 using artificial neural networks.* Corrosion Science, 2015. **92**: p. 217-227.
108. Sun, Y., et al., *Development of constitutive relationship model of Ti600 alloy using artificial neural network.* Computational Materials Science, 2010. **48**(3): p. 686-691.
109. Hasan, M.H., et al., *ANN modeling of nickel base super alloys for time dependent deformation.* Journal of Automation and Control Engineering Vol, 2014. **2**(4).
110. Sarkar, A., et al., *Artificial neural network modelling of in-reactor diametral creep of Zr2. 5% Nb pressure tubes of Indian PHWRs.* Annals of Nuclear Energy, 2014. **69**: p. 246-251.
111. Chakravartty, J., R. Singh, and A. Sarkar, *Assessment of Deformation Behavior of Zr-2.5 Nb Alloy during Thermo-Mechanical Processing and under Service Condition.* Procedia Engineering, 2013. **55**: p. 685-692.
112. Lu, Q., S. van der Zwaag, and W. Xu, *Charting the 'composition–strength'space for novel austenitic, martensitic and ferritic creep resistant steels.* Journal of Materials Science & Technology, 2017. **33**(12): p. 1577-1581.
113. Hou, J., et al., *Effect of hafnium on creep behavior of a corrosion resistant nickel base superalloy.* Materials Science and Engineering: A, 2010. **527**(6): p. 1548-1554.
114. Linn, S., et al., *Evaluation of property scatter of Ni-base alloy in 738 LC.* Materials Science and Engineering: A, 2011. **528**(13-14): p. 4676-4682.
115. Lu, Q., S. van der Zwaag, and W. Xu, *High-throughput design of low-activation, high-strength creep-resistant steels for nuclear-reactor applications.* Journal of Nuclear Materials, 2016. **469**: p. 217-222.
116. Srinivasan, V., et al., *Low cycle fatigue and creep–fatigue interaction behavior of 316L (N) stainless steel and life prediction by artificial neural network approach.* International Journal of Fatigue, 2003. **25**(12): p. 1327-1338.
117. Vishnu, P., N.S. Kumar, and M. Manohar, *Performance prediction of electric discharge machining of Inconel-718 using artificial neural network.* Materials Today: Proceedings, 2018. **5**(2): p. 3770-3780.
118. Adithiyaa, T., D. Chandramohan, and T. Sathish, *Optimal prediction of process parameters by GWO-KNN in stirring-squeeze casting of AA2219 reinforced metal matrix composites.* Materials Today: Proceedings, 2020. **21**: p. 1000-1007.

119. Pouraliakbar, H., et al., *Artificial neural networks for hardness prediction of HAZ with chemical composition and tensile test of X70 pipeline steels.* Journal of Iron and Steel Research International, 2015. **22**(5): p. 446-450.
120. Lakshminarayanan, A. and V. Balasubramanian, *Comparison of RSM with ANN in predicting tensile strength of friction stir welded AA7039 aluminium alloy joints.* Transactions of Nonferrous Metals Society of China, 2009. **19**(1): p. 9-18.
121. Thankachan, T., et al., *Prediction of surface roughness and material removal rate in wire electrical discharge machining on aluminum based alloys/composites using Taguchi coupled Grey Relational Analysis and Artificial Neural Networks.* Applied Surface Science, 2019. **472**: p. 22-35.
122. Garg, A. and J.S.L. Lam, *Modeling multiple-response environmental and manufacturing characteristics of EDM process.* Journal of Cleaner Production, 2016. **137**: p. 1588-1601.
123. Yadav, S.K., *Optimization of green electro-discharge machining using VIKOR*. 2013.
124. Farley, S.J., et al., *High resolution non-destructive evaluation of defects using artificial neural networks and wavelets.* Ndt & E International, 2012. **52**: p. 69-75.

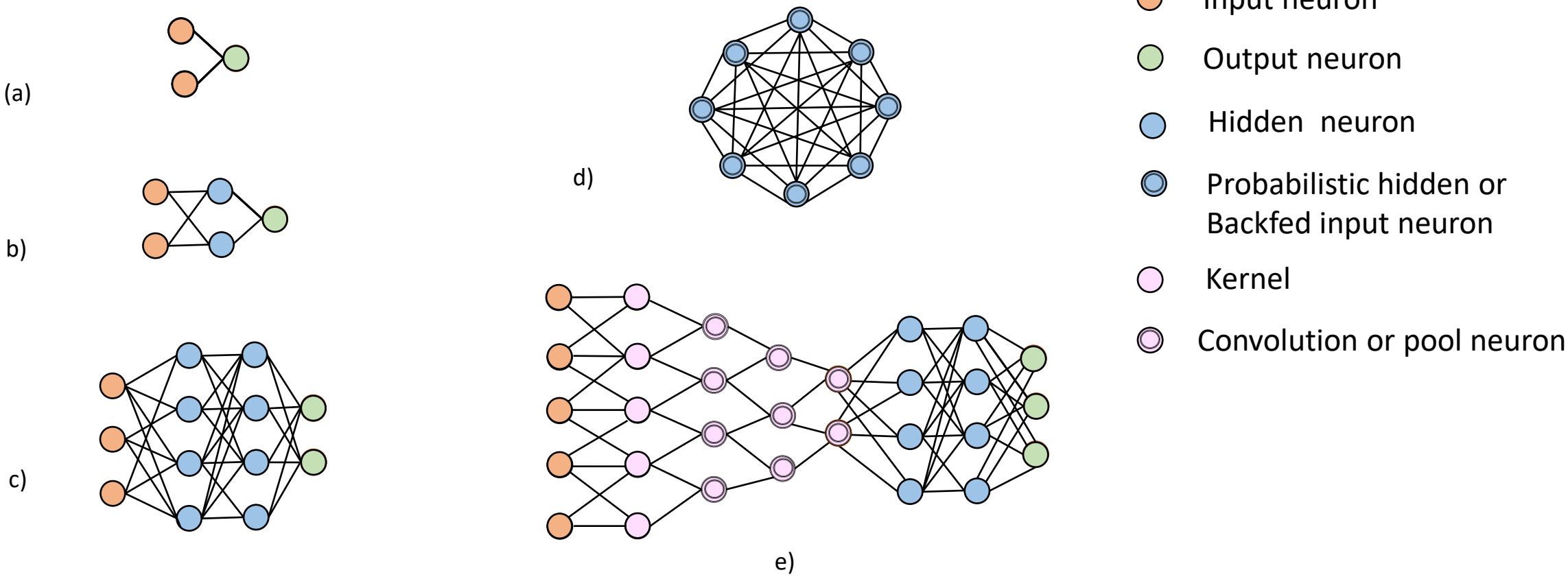


Figure 1 Some neural network architecture (a) Perceptron (b) Multilayer perceptron, Radial basis network (c) Deep Feed Forward (DFF) neural network (d) Markov Chain (MC), Hopfield Network (HN), Boltzmann Machine(BM), (e) Deep Convolutional Network (DCN) (after Van Veen [8]).

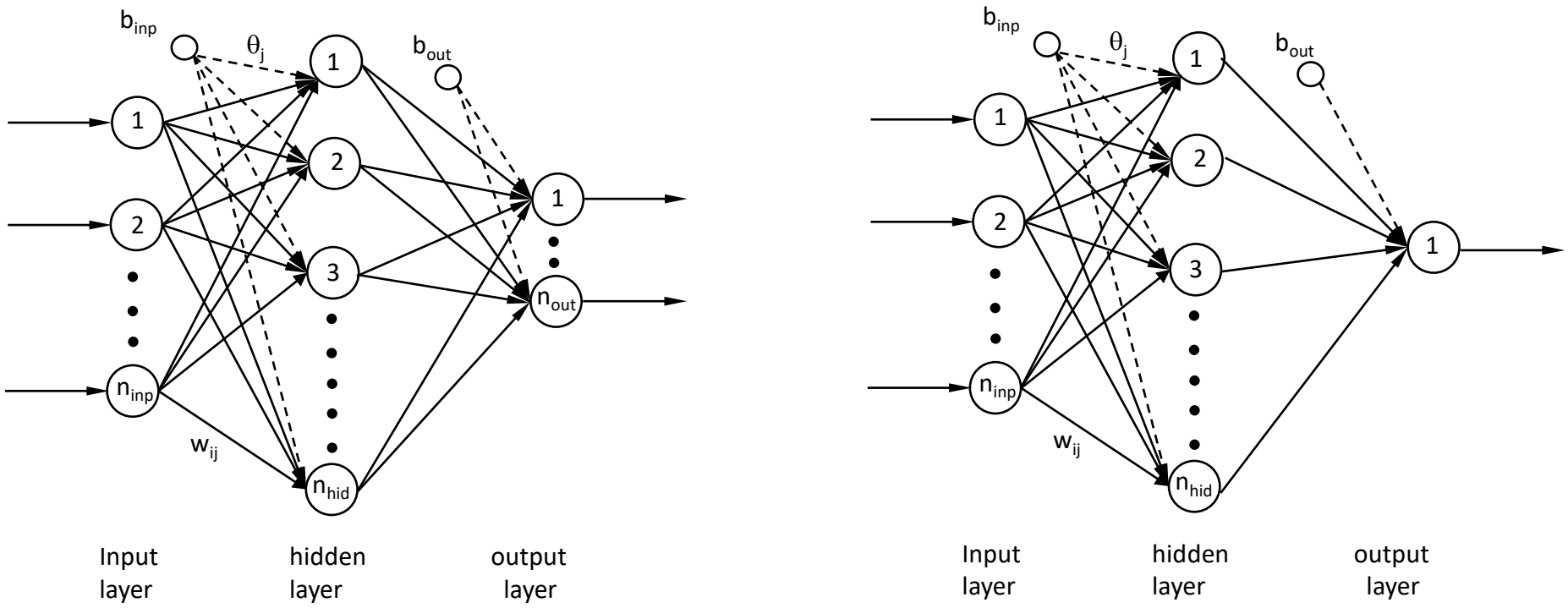


Figure 2 Multilayer feed forward neural network with more details of configuration

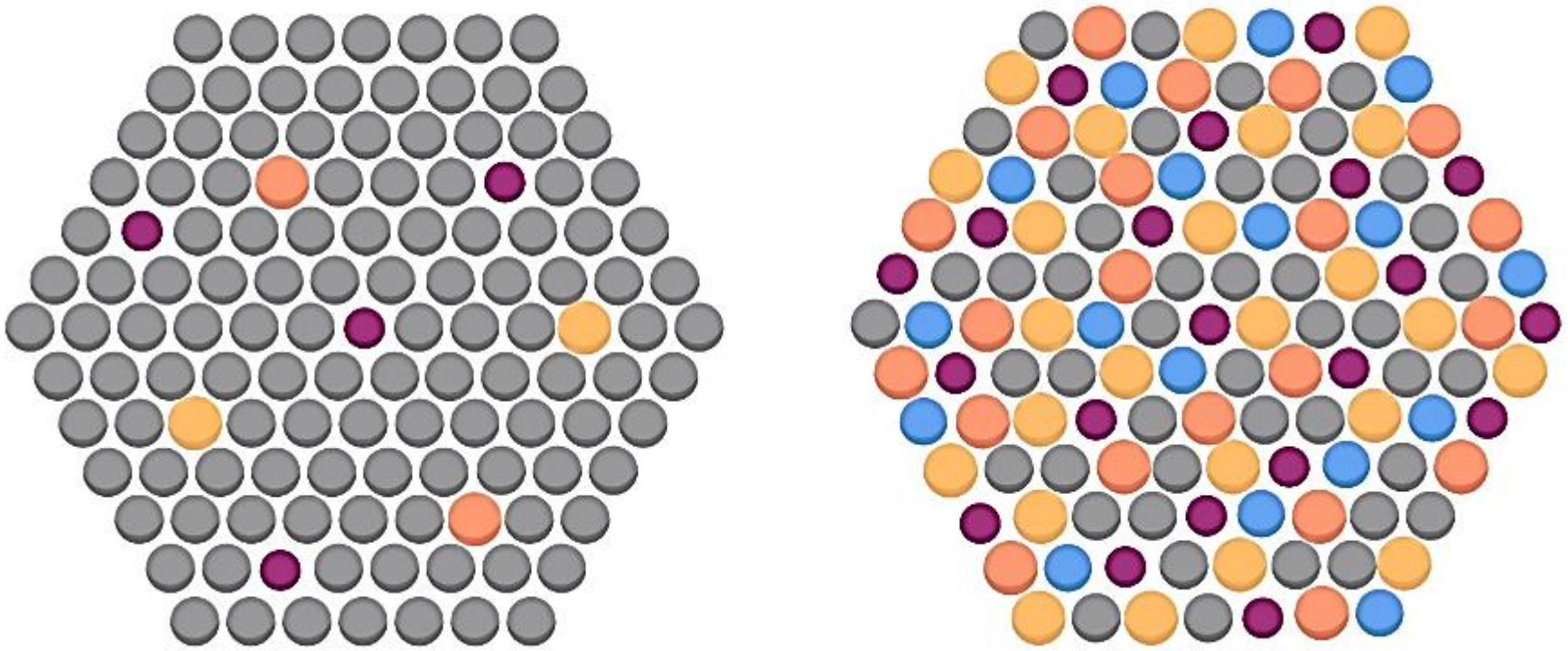

(a) (b)

Figure 3 Illustrations of structures of (a) Conventional and (b) High-entropy alloys with different colours and sizes representing different atoms (after Gorse et al [34]).

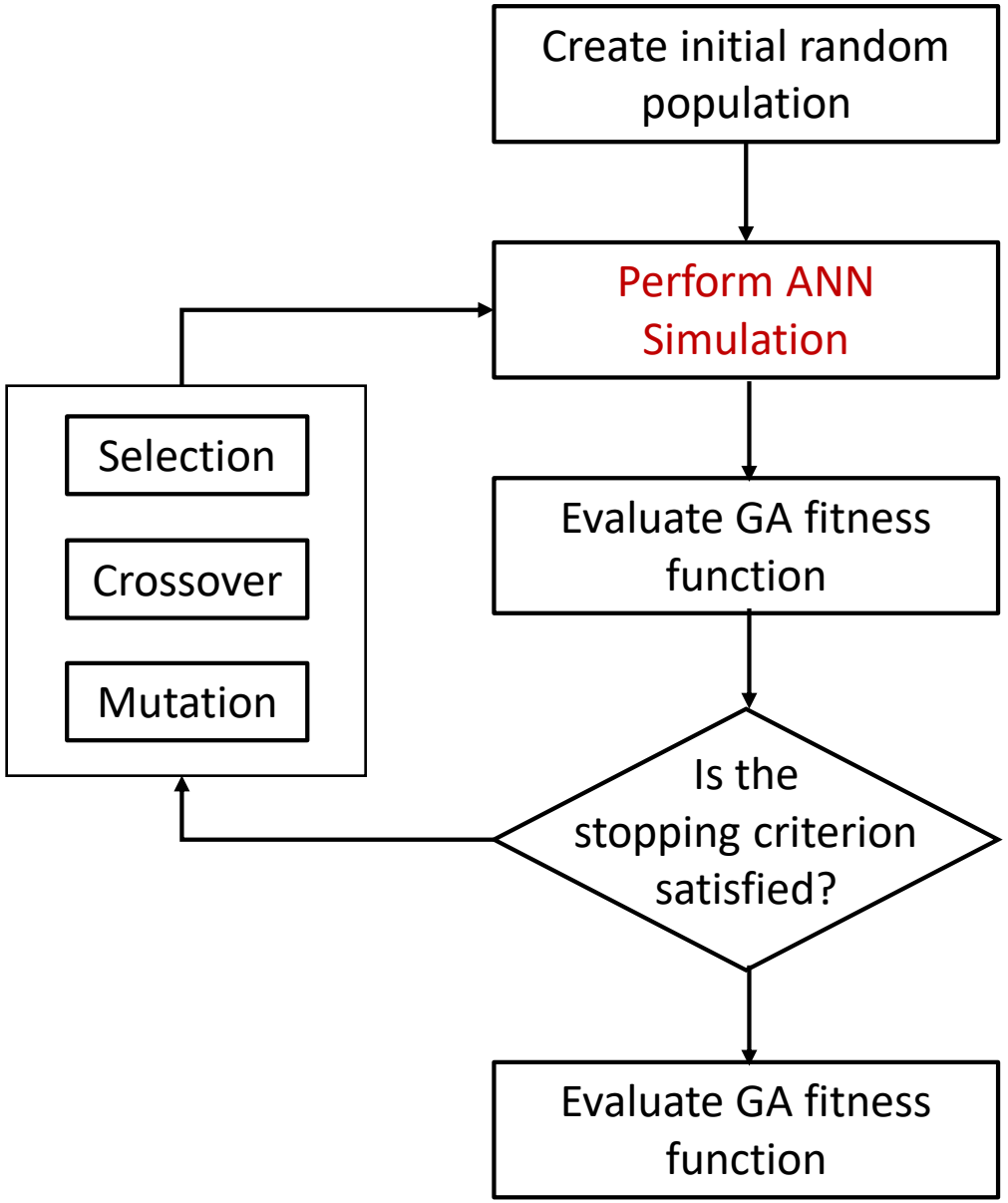


Figure 4 Flow chart of GA based optimization model (after Sun et al [41]).

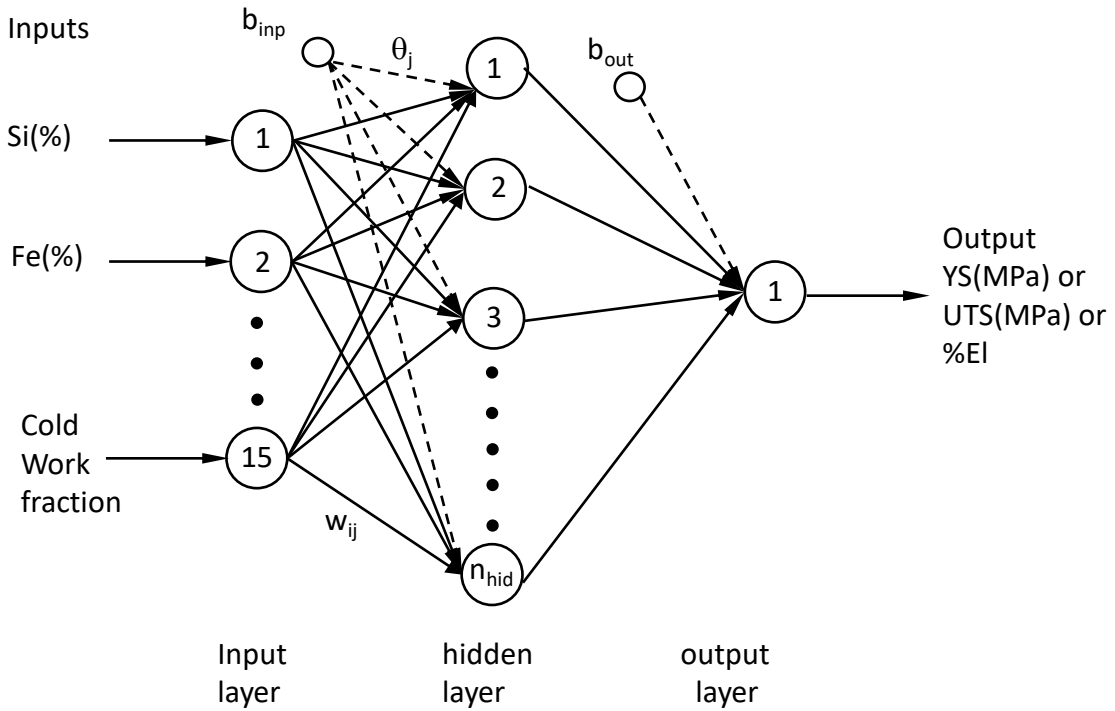


Figure 5 Illustration of multilayer feed forward neural network for mechanical properties.

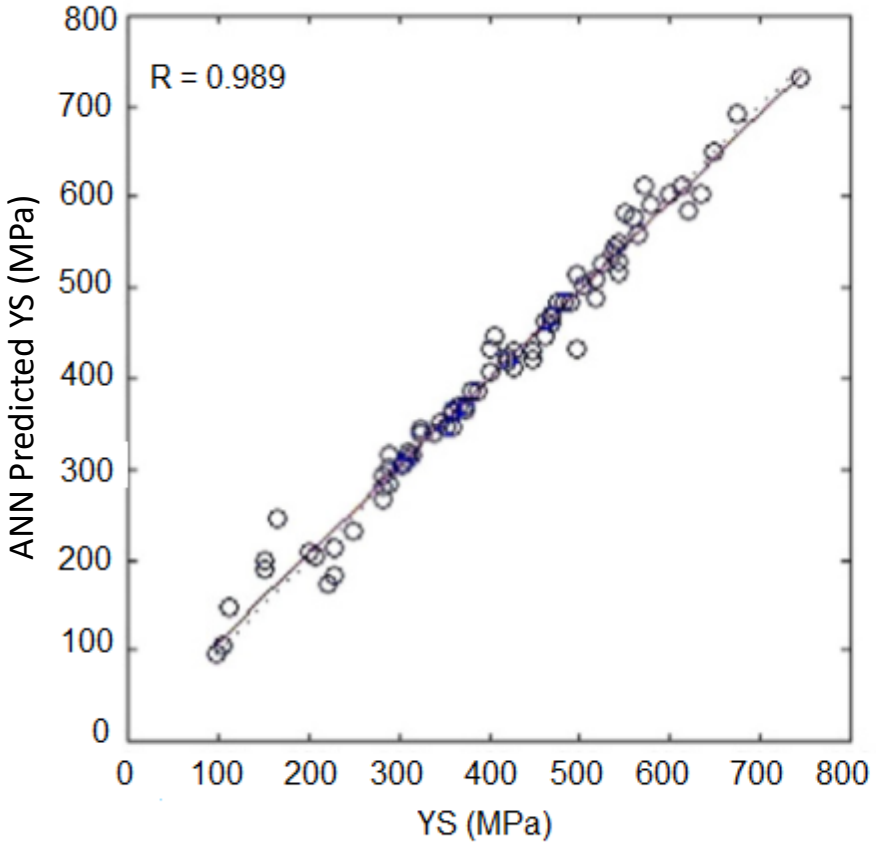


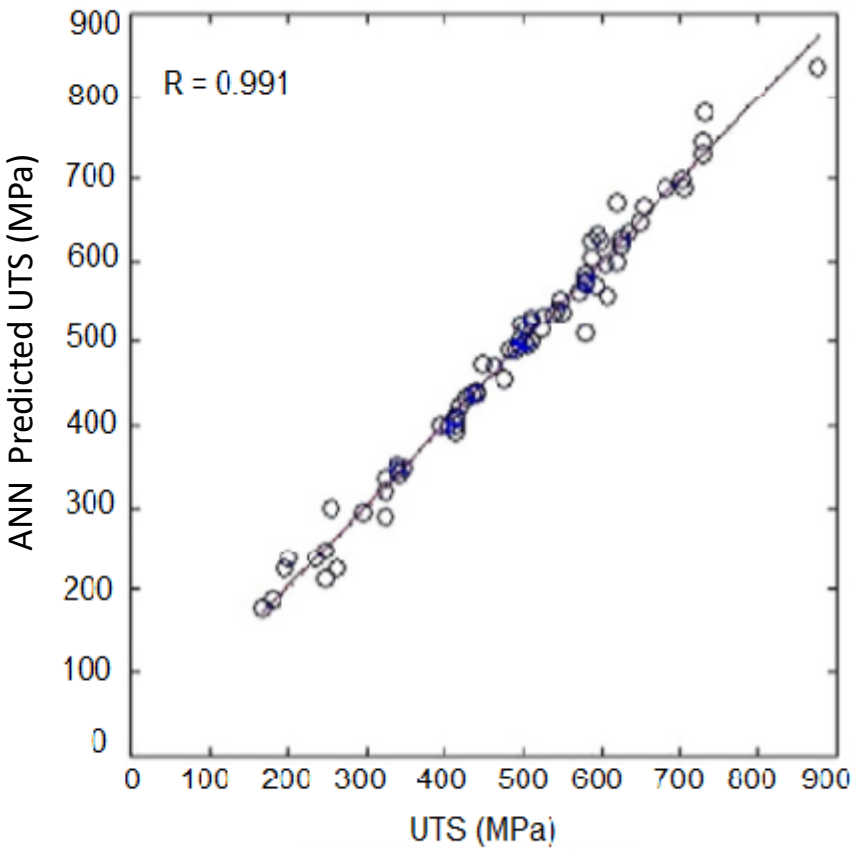


Figure 6 plots of a) Yield stress YS and b) ultimate tensile stress UTS predicted using trained ANN model against experimental values from [42] (after Dey et al [40]). .

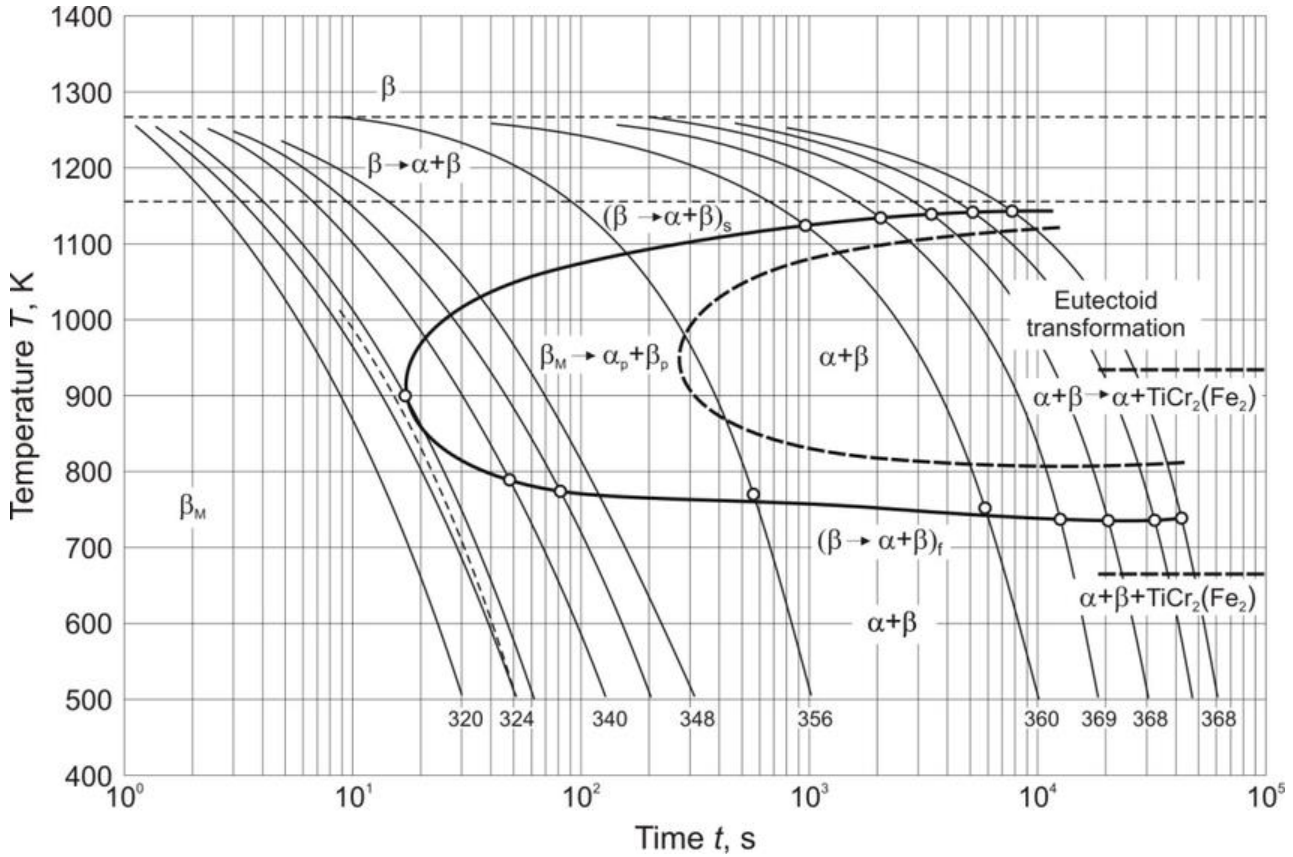


Figure 7 An example of a continuous cooling transformation diagram for a Ti-6Al-5Mo-5V-1Cr-1Fe alloy (AFTER Sieniawski et al [54]).

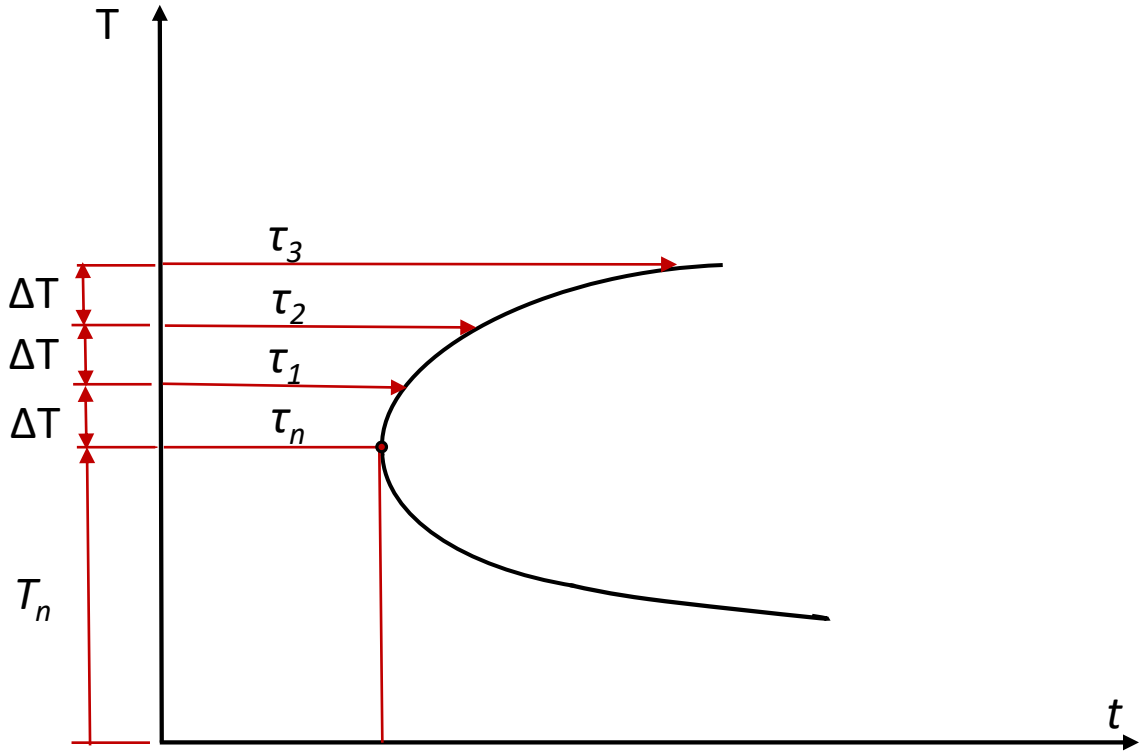


Figure 8 Description of target points on the TTT diagram, *T*-Temperature, *t* – time, (after Malinov et al [55]).

| | | |
|---|---|---|
| Supervised Learning | Classification | • Support Vector Machines<br>• Binary Decision trees<br>• Discriminant Analysis<br>• Nearest Neighbours<br>• Naïve Baysian<br>• Neural Network<br>• Deep Neural Networks |
| | Regression | • Neural Network<br>• Decision Trees<br>• Deep Neural Network |
| Unsupervised Learning | Policy iteration | • Monte Carlo<br>• Temporal Difference |
| | Value Iteration | • Q-learning |
| Reinforcement learning | Clustering | • K - means<br>• PCA<br>• Spectral clustering<br>• Hdden Markov<br>• Dirichlet process<br>• Neural Networks |
| | Dimensionality reduction | • PCA<br>• Auto-associative Neural Network<br>• Isometric Feature Mapping |
| | Density estimation | • Boltzamann Machine<br>• Kernel Density<br>• Gaussian Mixtures |

Table 1 Classification of Machine Learning (ML) Methods